FEBS Letters 478 (2000) 166–172 FEBS 23951

Overexpression of T-type calcium channels in HEK-293 cells increases intracellular calcium without affecting cellular proliferation

Jean Chemin[a], Arnaud Monteil[a], Christelle Briquaire[a], Sylvain Richard[a], Edward Perez-Reyes[b], Joël Nargeot[a], Philippe Lory[a,*]

[a] *IGH-CNRS UPR 1142-141, rue de la Cardonille, F-34396 Montpellier Cedex 05, France*
[b] *Department of Pharmacology, University of Virginia, 1300 Jefferson Park Avenue, Charlottesville, VA 22908, USA*

Received 10 May 2000; revised 28 June 2000; accepted 28 June 2000

Edited by Maurice Montal

Abstract Increased expression of low voltage-activated, T-type Ca^{2+} channels has been correlated with a variety of cellular events including cell proliferation and cell cycle kinetics. The recent cloning of three genes encoding T-type α_1 subunits, α_{1G}, α_{1H} and α_{1I}, now allows direct assessment of their involvement in mediating cellular proliferation. By overexpressing the human α_{1G} and α_{1H} subunits in human embryonic kidney (HEK-293) cells, we describe here that, although T-type channels mediate increases in intracellular Ca^{2+} concentrations, there is no significant change in bromodeoxyuridine incorporation and flow cytometric analysis. These results demonstrate that expressions of T-type Ca^{2+} channels are not sufficient to modulate cellular proliferation of HEK-293 cells.

Key words: Calcium channel; T-type; Calcium imaging; Proliferation; Flow cytometry; HEK-293 cell

1. Introduction

T-type Ca^{2+} channels (T-channels) are preferentially expressed at foetal and early developmental stages of neuronal and muscle cells [1–4] and a high level of T-channel expression is observed in early mouse embryos [5] and blastocyst-derived embryonic stem cells [6]. In cultured smooth muscle cells, it has been described that the expression of T-channels is transient and parallels cell proliferation [7]. Recently, combined patch-clamp and immunocytochemistry techniques have shown a correlation between functional T-channels and the presence of specific markers of the cell cycle, both in cultured smooth muscle cells [8] and in cardiomyocytes [9]. Similarly, many proliferating cell lines exhibit large T-type current ($I_{Ca,T}$) [10,11]. However, the fundamental question of whether a rise in T-channel expression is a trigger or a consequence of cell proliferation still remains. The use of mibefradil, a T-channel blocker, has suggested that $I_{Ca,T}$ is a trigger of cellular proliferation [12]. Unfortunately, mibefradil is not a specific blocker of T-channels since it affects high voltage-activated Ca^{2+} channels and other ionic channels [13], or even cytochrome *P*-450 [14]. Consequently, proof that T-channels mediate proliferation may be provided by the manipulation of T-channel expression in proliferating cells since several α_1 subunits encoding T-channels have been cloned [4,15–19].

In the present study, we have examined whether overexpression of T-channels generated by the human α_{1G} and α_{1H} subunits modulates proliferation and cell cycle kinetics of the human embryonic kidney (HEK-293) cell line. Functional expression studies in this cell line have already been used successfully to study proliferation [20–22], as well as Ca^{2+} channel-dependent gene expression [23]. Recently, it was shown that recombinant T-channels generated by the α_{1G} and α_{1H} subunits exhibit in HEK-293 cells similar properties to those described in native cells [4,16]. We describe here that functional expression of T-channels, which increases basal intracellular Ca^{2+} concentration, does not induce any change in proliferation and cell cycle kinetics.

2. Materials and methods

2.1. Cell culture, transfection and isolation of cell lines

Twenty-four hours before transfection, HEK-293 cells were plated at 70–90% confluence in 35-mm dishes (Nunc) and grown in Dulbecco's modified Eagle's medium (Eurobio) supplemented with 10% foetal bovine serum (Eurobio) and 1% penicillin–streptomycin (Gibco). A human α_{1G} cDNA (α_{1G-b} [4]) subcloned into pBK-CMV vector (Stratagene), as well as control pBK-CMV and pcDNA3 vectors, were transfected using the standard calcium phosphate procedure. To establish cell lines, 1 mg/ml G418 (Life Technologies) was added to the culture medium 48 h after transfection. After 7–10 days of G418 treatment, cells transfected with the pBK-CMV-α_{1G} construct were trypsinised and plated at a clonal density in a 96-well dish and expanded. The resulting stable transfectants were screened for $I_{Ca,T}$ with electrophysiological techniques (see Section 2.2) and positive colonies were maintained in G418 selection. Construction of the stable HEK-293 cell line, AH13, which overexpressed the human α_{1H} (pcDNA3-α_{1H}) was described previously [16]. In order to doublecheck the role of the backbone vectors, the cDNA encoding α_{1H} was also subcloned into the pBK-CMV vector. In transient transfection experiments, cells were co-transfected with an expression vector encoding the green fluorescent protein (GFP) directed to the plasma membrane (pBB14: a generous gift from L.W. Enquist, [24,25]). GFP was used to monitor the transfection efficiency (70% in average) and to identify positive cells in electrophysiological and Ca^{2+} imaging experiments in which the pBKCMV-α_{1H} or pBKCMV-α_{1G} constructs were cotransfected in a 10:1 ratio with the GFP construct.

2.2. Electrophysiology

The recording of whole-cell currents in HEK-293 cells overexpressing α_{1G} and α_{1H} channels and their analysis were achieved as described elsewhere [4,16]. The extracellular solution contained (in mM): 2 $CaCl_2$, 160 TEACl and 10 HEPES (pH to 7.4 with TEAOH). Pipettes made of borosilicate glass with a typical resistance of 1–2 MΩ were filled with an internal solution containing (in mM): 110 CsCl, 10 EGTA, 10 HEPES, 3 Mg-ATP and 0.6 Na-GTP (pH to 7.2 with

*Corresponding author. Fax: (33)-499-61 99 01.
E-mail: philippe.lory@igh.cnrs.fr

Abbreviations: $I_{Ca,T}$, T-type current; BrdU, bromodeoxyuridine; HU, hydroxyurea; VSM, vascular smooth muscle

0014-5793/00/$20.00
PII: S0014-5793(00)01832-9

CsOH). The resting membrane potential (RMP) of HEK-293 cells was measured in whole-cell configuration immediately after breaking the patch membrane with an external medium made of Locke buffer containing (in mM): 140 NaCl, 5 KCl, 1.2 KH_2PO_4, 1.2 $MgSO_4$, 2 $CaCl_2$, 10 glucose and 10 HEPES (pH 7.2), and pipette filled with (in mM): 110 K-aspartate, 20 KCl, 8 NaCl, 1 $MgCl_2$, 1 $CaCl_2$, 10 EGTA, 10 HEPES, 4 Mg-ATP, 0.3 Tris–GTP and 14 creatine phosphate (pH to 7.3 with KOH). In these experiments, the junction potential was less than 3 mV. Activation and inactivation curves were obtained using Boltzmann equations and the negative product of these two curves generated a theoretical 'window' current described earlier [4]. The results are presented as the mean ± S.E.M., and *n* is the number of cells used.

2.3. Calcium imaging

Twenty-four hours after transfection, cells were trypsinised and plated onto polyornithine-coated borosilicate chambers (lab-tek; Nunc) and cultured for 24 h. For the measurement of intracellular Ca^{2+}, cells were incubated with 2.5 μM of acetoxymethyl ester of the dual-excitation ratiometric Ca^{2+} sensitive indicator fura-2 (Molecular Probes) at 37°C in the dark for 30 min in Locke buffer. Cells were then washed thoroughly in Locke buffer and mounted onto the stage of an inverted microscope (Olympus IX70) equipped with epifluorescence and interfaced with the MERLIN software (LSR, Cambridge, UK) to a monochromator (Spectramaster) and a 12/14 bit frame transfert rate digital camera (Astrocam). The MERLIN software was also used to calculate the 340/380 fluorescence ratio (Rf). The intensity for fluorescent light emission ($\lambda = 510$ nM) using excitation at 340 and 380 nm was monitored at the level of each single fura-2-loaded cell of the field. Extracellular application of Locke buffer containing various concentrations of KCl (5 and 40 mM, substituted with NaCl), Ca^{2+} (0, 2 and 5 mM, substituted with $MgCl_2$), mibefradil (1 μM), nickel ($NiCl_2$) and ATP (20 μM) was achieved using a gravity-driven multiple perfusion system placed in the close proximity of the cells studied. In order to estimate the intracellular Ca^{2+} concentration from ratio images, calibration of the fura-2 fluorescence was performed in ionomycin-treated HEK-293 cells (10 μM) incubated in the presence (5 mM) and in the absence (0 mM plus 10 mM EGTA) of external Ca^{2+}. The estimated $[Ca^{2+}]_{in}$ was deduced from the equation: $[Ca^{2+}] = K_d(f_{380\ min}/f_{380\ max})(Rf-Rf_{min})/(Rf_{max}-Rf)$, where K_d was 225 nM and Rf_{min} (0.5∼0.6 range) and Rf_{max} (1.4∼1.6 range) are the Rf values when the dye is free of Ca^{2+} (0 Ca^{2+}/EGTA) and saturated with Ca^{2+} (5 mM Ca^{2+}), respectively. Data are presented as mean ± S.E.M. and statistical analyses are performed with the Student's *t*-test.

2.4. Bromodeoxyuridine (BrdU) labeling

For BrdU labeling, stable cells were plated at 30% confluence on 12-mm glass coverslips in 35-mm Petri dishes. After 48 h, 10 μM BrdU (Roche) was added to the medium for 45 min. Control experiments with 2 mM hydroxyurea (HU; Sigma) were performed using non-transfected cells maintained for 48 h in the presence of HU and treated with BrdU still in the presence of HU (+HU, Fig. 3) or just after removal of HU (−HU, Fig. 3). BrdU-treated cells were rinsed with phosphate-buffered saline (PBS) and fixed at room temperature for 5 min in a 3.7% formaldehyde solution (Sigma) and washed with PBS. Cells were permeabilised using cold acetone for 30 s, washed twice (H_2O and PBS) and treated with 3 N HCl for 15 min. After several washes with H_20 and PBS, the blocking of non-specific sites was performed by incubating cells at 37°C in a 1% PBS–bovine serum albumin (BSA) solution for 30 min. Cells were then incubated for 30 min at 37°C with a mouse anti-BrdU antibody (Amersham), washed three times with PBS and incubated with a sheep anti-mouse biotinylated antibody (Amersham) at 1/100 dilution in PBS–BSA solution during 50 min at 37°C. After three PBS washes, cells were treated for 30 min at 37°C with a streptavidin Texas Red antibody (Amersham) at 1/200 dilution in 1% PBS–BSA solution. Cells were finally washed (3× PBS and H_2O), labeled for 1 min with Hoescht 33258 nuclear dye (Sigma) and the coverslips were mounted using Gelmount (Biomedia). Digital images were acquired on a microscope (Leica) and analysed with Adobe Photoshop 4.0. The percentage of proliferative cells was defined as the ratio of BrdU and Hoescht-positive cells (taken in a minimum of 10 independent fields). Results are presented as the mean ± S.E.M. and *n* is the number of independent transfections.

2.5. Flow cytometry

For this set of experiments HEK-293 cells were plated at 90% confluence on 35-mm Petri dishes from an initial large scale culture 1 day before transfection. Transfection was achieved using Fugene 6TR (Roche) to avoid cell cycle modulation observed with Ca^{2+} phosphate transfection procedure. Twenty-four hours after the transfection, cells were trypsinised from each 35-mm dish and redistributed on three 60-mm dishes at low density (10% confluence). After 3 days, cells were collected by trypsinisation, pelleted and resuspended in PBS. Two volumes of cold, absolute ethanol were added and the samples were stored at −20°C. For cell cycle analysis, cell samples were pelleted and resuspended in staining solution (25 μg/ml propidium iodide, 0.1% trisodium citrate dihydrate, 100 μg/ml RNAse A, 0.05 mM EDTA, 0.1% Triton X-100). Samples were maintained at 4°C for at least 2 h in the dark prior to analysis. Flow cytometric analysis was performed using a FACscan (Becton Dickinson Immunocytometry System) and analysed using Modfit LT software (Verity Software House). Data are presented for each phase of the cell cycle as the mean ± S.E.M., and *n* is the number of independent transfections used.

3. Results

Whole-cell recordings of $I_{Ca,T}$ were performed to verify that both α_{1G} and α_{1H} subunits led to functional expression of recombinant T-channels in HEK-293 cells both in transient and stable cell lines (Fig. 1). Fig. 1A,B present typical families of fast inactivating $I_{Ca,T}$ generated by recombinant α_{1G} and α_{1H} channels, respectively, that were obtained on stable cell lines. The averaged current–voltage relationships (Fig. 1C,D, respectively) exemplify that these two subunits produce typical low voltage-activated currents, as described recently [4,16]. Steady-state activation properties (Fig. 1E,F) were similar both for α_{1G} and α_{1H} currents considering the potential for half-activation (−45.5 ± 1.2 mV, $n = 10$ and −47.7 ± 1 mV, $n = 10$, respectively), while the potential for half-inactivation ($V_{0.5}$) was significantly different ($P < 0.05$, Student's *t*-test) for α_{1G} (−66 ± 0.6 mV, $n = 6$) and α_{1H} (−72.5 ± 0.4 mV, $n = 6$) currents. Superimposition of steady-state activation and inactivation curves revealed the existence of a window current both for the α_{1G} and α_{1H} currents (Fig. 1E and F). When plotted as a function of the membrane potential, the predicted window currents for α_{1H} and α_{1G} channels peaked at −65 and −48 mV, respectively (Fig. 1G,H). The RMP of control HEK-293 cells measured in Locke buffer was −35 ± 5 mV ($n = 11$, not shown), with the more hyperpolarised cells having a RMP around −50 mV (∼30% of the cells). Altogether, these electrophysiological data clearly indicated that HEK-293 cells expressed functional recombinant T-channels and suggested that these channels could contribute to a moderate and constant Ca^{2+} entry at the cell's RMP.

We then investigated whether overexpression of recombinant T-channels lead to detectable changes in intracellular Ca^{2+} concentration. HEK-293 cells were loaded with fura-2 and analysed as described in Section 2. A typical experiment performed with control and α_{1H}-transfected cells is presented in Fig. 2A,B. External perfusion of Locke buffer containing various Ca^{2+} concentrations (0, 2 and 5 mM) induced significant changes in the intracellular Ca^{2+} concentration in transfected cells (99 ± 5, 125 ± 4 and 164 ± 11 nM, respectively, $n = 11$) (Fig. 2B), but not in control HEK-293 cells (116 ± 2, 115 ± 2 and 119 ± 3 nM, respectively, $n = 25$). Although these experiments indicate that significant variation of $[Ca^{2+}]_{in}$ can be observed in the presence of physiological external Ca^{2+} concentration (2 mM), we used a Locke medium containing 5 mM Ca^{2+} which increases the driving force and thereby

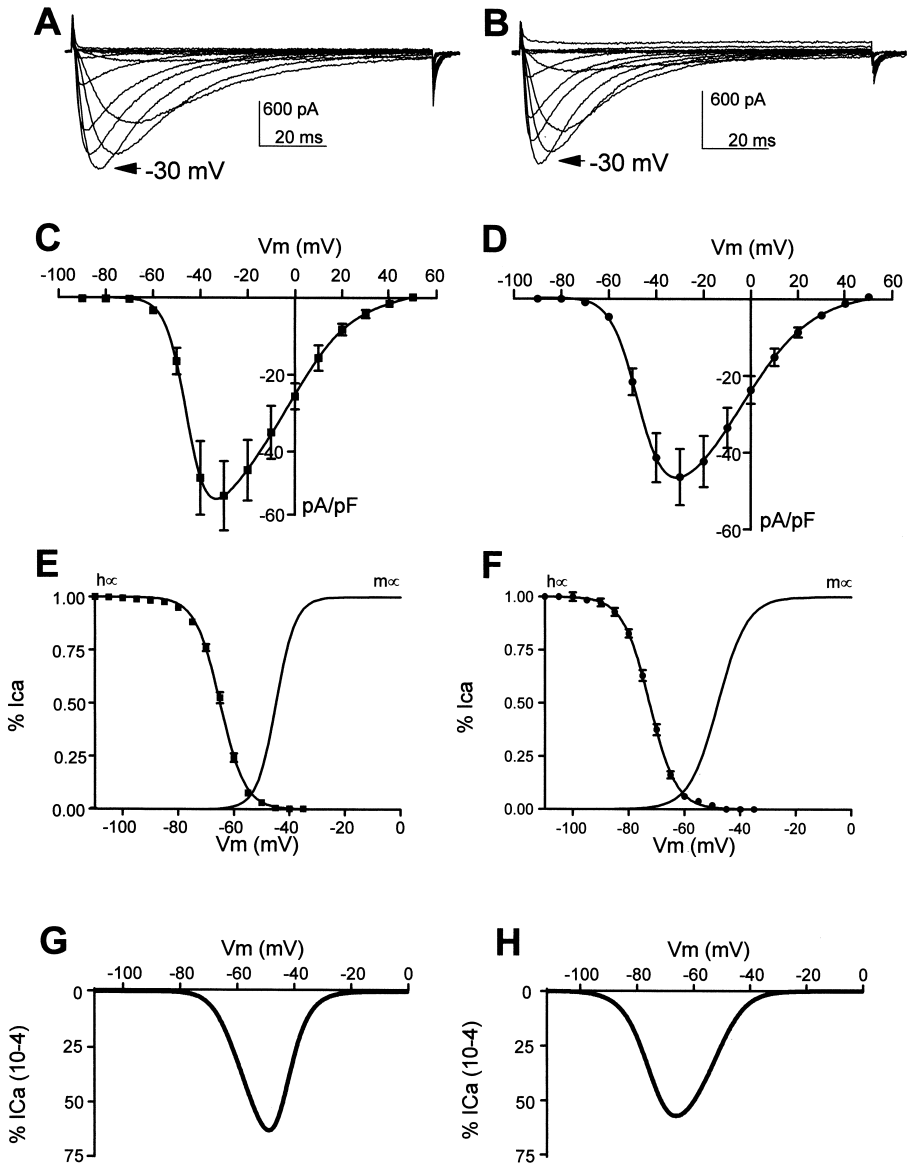

Fig. 1. Electrophysiological properties of Ca^{2+} currents ($I_{Ca,T}$) generated by α_{1G} and α_{1H} subunits. A and B: Representative whole-cell Ca^{2+} currents recorded in a cell transfected with pBK-CMV-α_{1G} and with pcDNA3-α_{1H}, respectively. The current traces were obtained for 100-ms depolarising pulses ranging from −90 to +50 mV, from a holding potential of −110 mV. The maximum current activation is obtained for a depolarising pulse at −30 mV (arrow) in both experimental situations. C and D: Averaged current–voltage relationships for α_{1G} current ($n=10$) and α_{1H} current ($n=10$), respectively. The maximum current amplitude for each depolarising step was measured from current traces as obtained in (A) and (B). The current density was calculated by dividing the current amplitude by the cell capacitance and plotted versus the test pulse value. E and F: Voltage-dependence of the activation and inactivation of α_{1G} current and α_{1H} current, respectively. Activation curves ($m\alpha$) were derived from the fit of the current–voltage curves as described in Section 2 ($n=10$). Similarly, inactivation curves ($h\alpha$), constructed from standard recordings using 5 s prepulses to various depolarising V_m were fitted with a Boltzmann function ($n=6$). Superimposed activation and inactivation curves predicted a window current. G and H: Calculated window current obtained by multiplying the activation conductance curve ($m\alpha$) by the inactivation curve ($h\alpha$) for α_{1G} current (G) and α_{1H} current (H), respectively. Considering the density of Ca^{2+} currents obtained in α_{1H} and α_{1G} expressing cells, the maximum window current density is 0.34 and 0.27 pA/pF, respectively.

favours the detection of intracellular Ca^{2+} variations in the experiments described below. It should be noted that electrophysiological experiments revealed that the switch from 2 to 5 mM of the external Ca^{2+} concentration induced a 45% increase in the current amplitude and a 4 mV shift in the steady-state activation and inactivation ($n=8$, not shown). The combined analysis of cells recorded from five independent transfections has clearly indicated that the basal intracellular concentration of Ca^{2+} ($[Ca^{2+}]_{in}$) in α_{1H}-transfected cells was markedly reduced by the application of mibefradil (1 μM) as well as by the removal of external Ca^{2+} (Fig. 2C), while no change was observed in control cells (Fig. 2D,E). Overall, cells transiently transfected with α_{1H} showed an average 340/380 ratio of fluorescence (R f340/f380) of 0.95 ± 0.03, corresponding to an estimated $[Ca^{2+}]_{in}$ of 198 ± 25 nM ($n=24$), which was significantly higher ($P=0.003$, unpaired Student's t-test) than the one recorded in control cells (0.81 ± 0.02, i.e. $[Ca^{2+}]_{in} = 126 \pm 14$ nM, $n=56$). In α_{1H}-transfected cells, the removal of external Ca^{2+} was associated with a significant decrease ($P=0.001$, paired Student's t-test) in the 340/380

ratio, from 0.95 ± 0.02 to 0.77 ± 0.01, i.e. 49% decrease in $[Ca^{2+}]_{in}$ from 198 ± 25 to 101 ± 14 nM ($n = 24$), but not in control cells ($[Ca^{2+}]_{in}$; 126 ± 14 and 120 ± 14 nM ($n = 56$), in 5 and 0 mM Ca^{2+}, respectively) (Fig. 2E). Basal $[Ca^{2+}]_{in}$ in α_{1H}-transfected cells was also strongly affected by Ni^{2+} concentrations as low as 5 μM (Fig. 2F), while in control cells no change in basal $[Ca^{2+}]_{in}$ was observed even in the presence of 300 μM Ni^{2+} (Fig. 2G). In addition, perfusion of 40 mM KCl

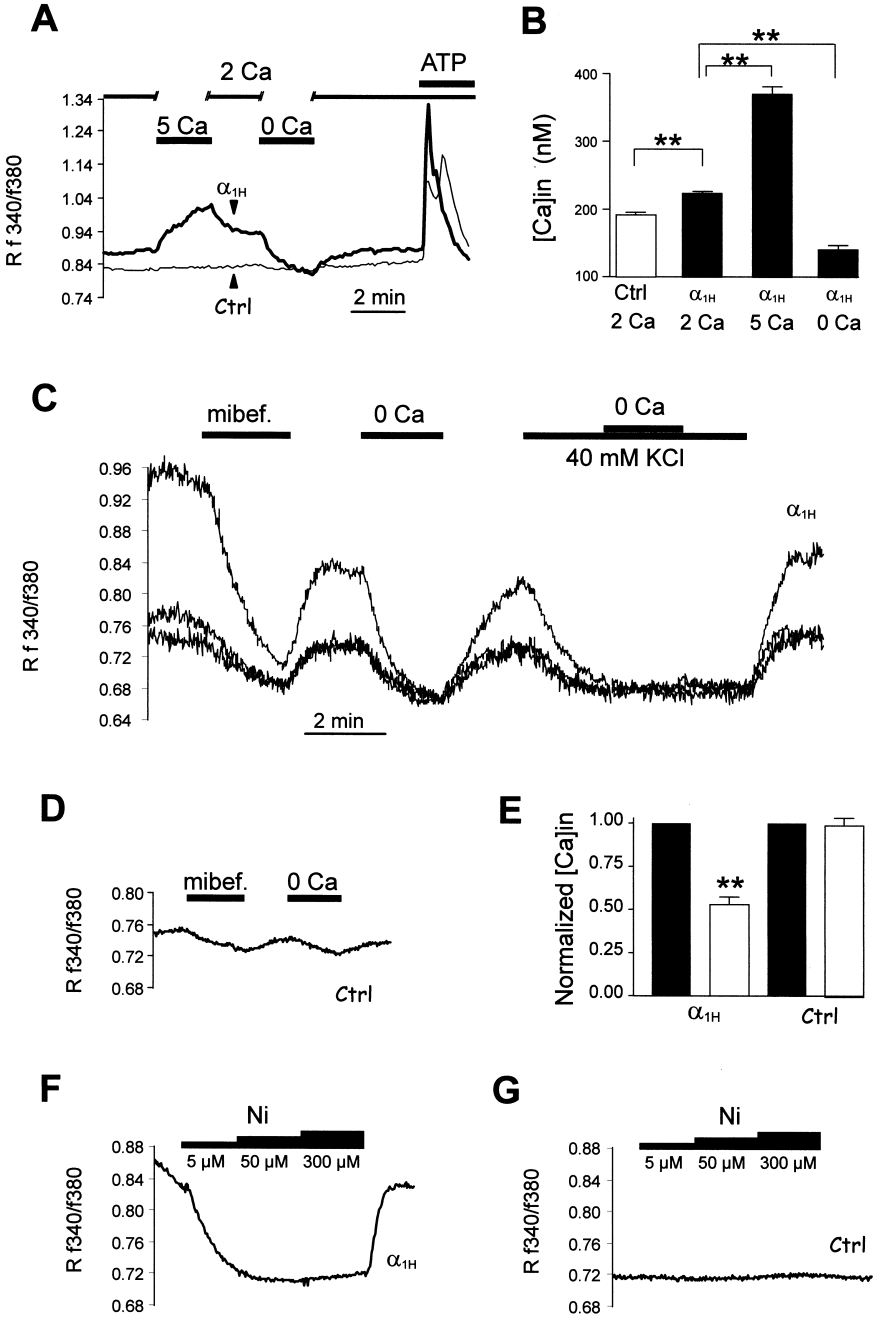

Fig. 2. Changes in $[Ca^{2+}]_{in}$ observed in HEK-293 cells overexpressing the α_{1H} subunit. A: α_{1H}-overexpressing (bold line, average of six cells) and control (normal line, average of five cells) cells were loaded with fura-2 and examined for their variation in $[Ca^{2+}]_{in}$ according to the ratio of fluorescence at 340 and 380 nm (R f340/f380) during perfusion of Locke medium containing 2, 5 and 0 mM Ca^{2+}. At the end of the experiment an application of ATP (20 μM) indicated the level of responsiveness of the cells. B: Histogram of the corresponding values of the $[Ca^{2+}]_{in}$ for control (white bar, $n = 25$) and α_{1H}-overexpressing cells (black bars, $n = 11$) in 2, 5 and 0 mM Ca^{2+}, as indicated in the figure. The changes in $[Ca^{2+}]_{in}$ that were significantly different at $P = 0.001$ (**) are indicated in the figure. C: α_{1H}-overexpressing cells were examined in the presence of 5 mM external Ca^{2+} following application of 1 μM mibefradil, removal of external Ca^{2+} (0 Ca) and application of 40 mM KCl, as indicated on the panel. The traces correspond to three individual cells. D: Average changes in $[Ca^{2+}]_{in}$ following application of 1 μM mibefradil and removal of external Ca^{2+} in control cells (average of five cells). E: Histogram representation of the changes in $[Ca^{2+}]_{in}$ following removal of external Ca^{2+} (white bars), compared to basal $[Ca^{2+}]_{in}$ (black bars) in α_{1H}-transfected cells (left part, $n = 24$) and in control cells (right part, $n = 56$). The change in $[Ca^{2+}]_{in}$ was significantly different at $P = 0.005$ (*) between control (5 mM Ca^{2+}) and 0 mM Ca^{2+} for α_{1H}-transfected cells. F: Change in basal $[Ca^{2+}]_{in}$ following application of 5, 50 and 300 μM Ni^{2+} in α_{1H}-transfected cells (average of five cells from one field). G: Similar experiment as in (D) on control cells (average of six cells from one field).

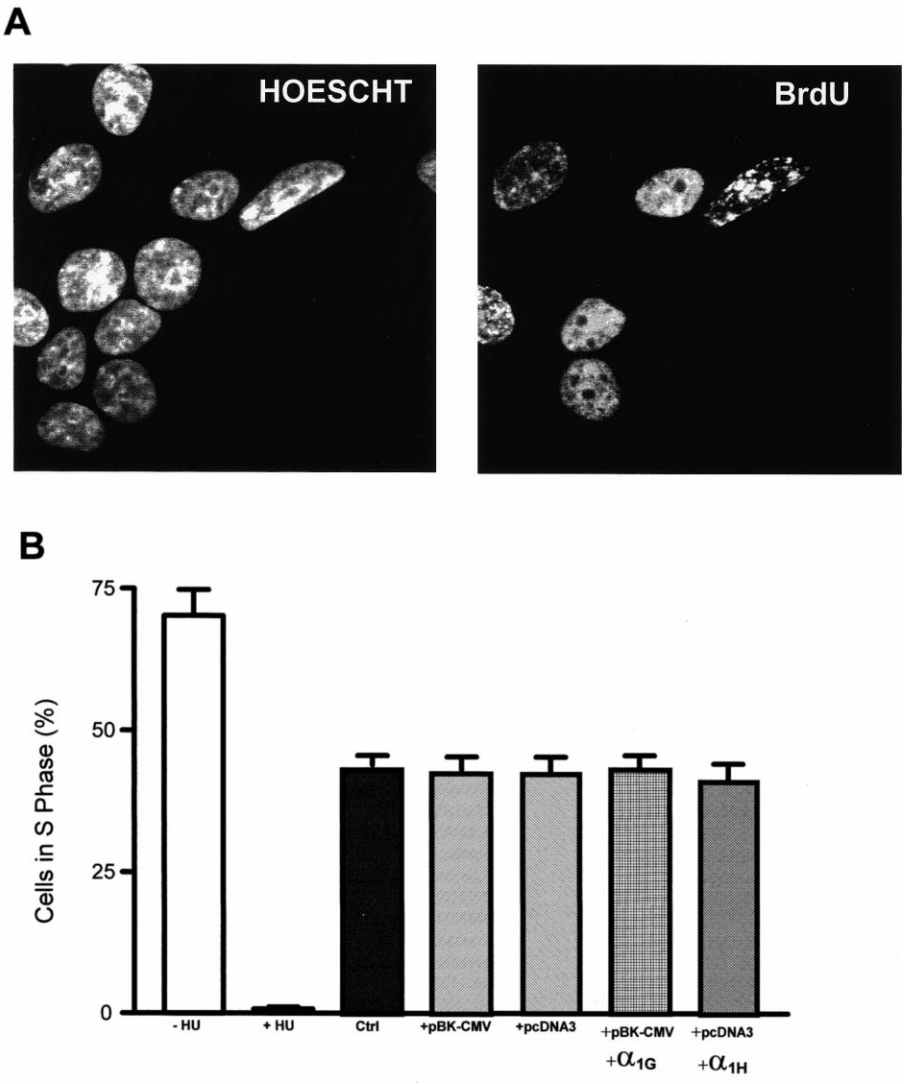

Fig. 3. Identification of BrdU-positive cells in control cell lines and in cell lines overexpressing T-channels. A: Example of a field showing cell nuclei stained with Hoescht 33258 (left panel) and BrdU (right panel). The staining procedures are described in Section 2. B: The bars (mean ± S.E.M.) represent the percentage of BrdU positive cells obtained from several independent transfections (see *n* values below) in a variety of experimental situations. The experimental situations are labeled as follow: −HU, HU is removed just before BrdU incubation in control cells cultivated for 48 h in the presence of HU ($n = 13$); +HU, HU is kept during the BrdU ($n = 24$); Ctrl, control HEK-293 cells ($n = 20$); +pBK-CMV, cell line established from HEK-293 cells transfected with the control vector ($n = 22$); +pcDNA3, cell line established from HEK-293 cells transfected with the control vector ($n = 12$); +pBK-CMV-α_{1G}, cell line established from HEK-293 cells transfected with the pBK-CMV-α_{1G} vector ($n = 28$); +pcDNA3-α_{1H}, cell line established from HEK-293 cells transfected with the pcDNA3-α_{1H} vector ($n = 14$).

which induces cell depolarisation also decreased the basal $[Ca^{2+}]_{in}$ in transfected cells (Fig. 2C). Removal of external Ca^{2+} in these experimental conditions did not contribute to an additional reduction of the basal $[Ca^{2+}]_{in}$. Similar results were obtained in cells transiently transfected with α_{1G} subunit, as well as for stable cell lines overexpressing α_{1G} or α_{1H} (not shown). Altogether, these data indicate that T-channels contribute to increase basal $[Ca^{2+}]_{in}$, most likely due to the existence of a window current.

The identification of $I_{Ca,T}$ and the concomitant evidence for an increase in basal $[Ca^{2+}]_{in}$ in cells overexpressing α_{1H} and α_{1G} subunits were important prerequisites for probing whether the proliferation of HEK-293 cells overexpressing T-type Ca^{2+} channels was affected. Using cell lines overexpressing the α_{1H} and α_{1G} subunits, we have performed BrdU labeling. BrdU is a thymidine analog and its incorporation into DNA during short incubation (45 min) is a good index of cell proliferation by identifying cells entering the S phase [26]. Control experiments were performed with cells incubated with 2 mM HU for 48 h which synchronises the cells in the G1/S transition. When cells were maintained in the presence of HU during BrdU incubation, no cell was BrdU positive, while the removal of HU before BrdU incubation led to 70% of the cells in S-phase. Nevertheless, no difference was observed between control HEK-293 cells (~40% in S-phase) and the cell lines overexpressing α_{1H} or α_{1G} subunits or the control vectors, pBK-CMV or pcDNA3, for their incorporation of BrdU (Fig. 3). In addition, BrdU incorporation after HU synchronisation of α_{1H} and α_{1G} cell lines gave similar results as for control cells suggesting that no change in the cell cycle kinetics was induced in cells overexpressing T-channels (not shown).

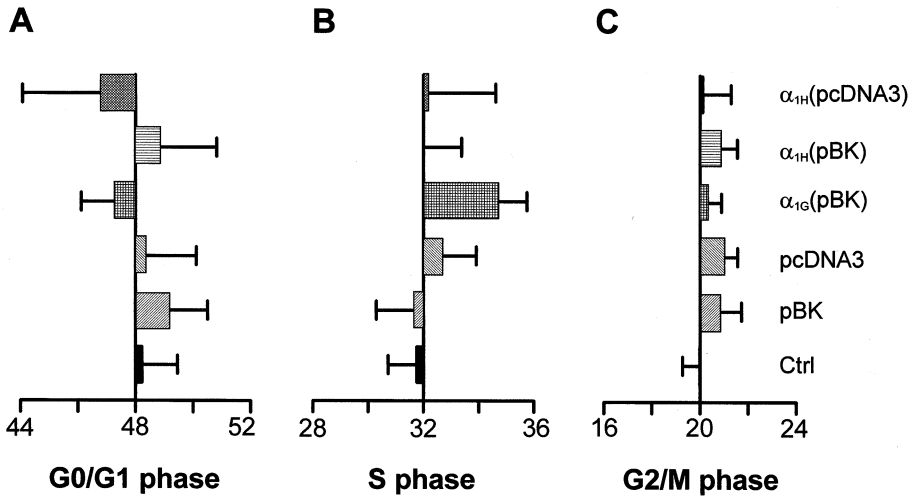

Fig. 4. Flow cytometric analysis of the percentage of cells in G0/G1, S and G2/M phases of the cell cycle in control cells and in cells overexpressing T-channels. Transiently transfected cells were counted following propidium iodide labeling as described in Section 2. The histograms are mean ± S.E.M. values scaled around the averaged values for G0/G1 phase (48%), S phase (32%) and G2/M phase (20%). The n value reported below represents the number of transfections for a variety of experimental conditions. The experimental conditions are mock-transfected cells (Ctrl, $n = 12$); pBK-CMV-transfected cells (pBK, $n = 13$); pcDNA3-transfected cells (pcDNA3, $n = 10$); pBK-CMV-α_{1G}-transfected cells (α_{1G} pBK, $n = 17$); pBK-CMV-α_{1H}-transfected cells (α_{1H} pBK, $n = 8$) and pcDNA3-α_{1H}-transfected cells (α_{1H} pcDNA3, $n = 10$).

We then used flow cytometry, a more specific approach, to detect whether overexpression of T-type calcium channels would modify cell cycle kinetics. We have designed this set of experiments using transiently transfected cells, whereas BrdU experiments described above were conducted on stable cell lines. Flow cytometric experiments were also performed with cells (i) incubated for 48 h with nocodazole and (ii) cells treated with HU following nocodazole treatment, to control the G2/M and G0/G1 peak analysis treatment. The fraction of cells in each phase of the cell cycle was then determined for various experimental conditions (Fig. 4). The percentage of control HEK-293 cells in G0/G1, S and G2M phases were 48.3 ± 1.1%, 31.8 ± 1% and 20 ± 0.5%, respectively. Similar results were obtained on the various samples of cells transfected with α_{1H} and α_{1G} cDNAs, on control plasmid-transfected cells, as well as on the stable transfected cell lines used above (not shown). The results presented in Fig. 4 were obtained from cells collected from at least 15 independent transfections. Overall, no significant differences in cell cycle activity were obtained among the various experimental conditions.

4. Discussion

The major finding of our study is that the functional expression of T-type Ca^{2+} channels in the HEK-293 cell line does not affect either proliferation or cell cycle kinetics. The data strongly suggest that the expression of T-channels by itself does not trigger a generalised signal transduction pathway that stimulates progression of the cell cycle. This study also describes for the first time that the basal level of $[Ca^{2+}]_{in}$ is increased in HEK-293 cells overexpressing T-channels. The dependence to extracellular Ca^{2+} ions and its sensitivity to mibefradil [4,16] and Ni^{2+} clearly indicate that T-type Ca^{2+} channels are involved in the regulation of the basal level of $[Ca^{2+}]_{in}$. Overexpression of the α_{1H} subunit was particularly useful in this demonstration since α_{1H} currents are blocked by low concentration of Ni^{2+} [27]. In addition, HEK-293 cells that overexpress T-channels do not elicit any Ca^{2+} transients following 40 mM KCl depolarisation, but a decrease in the basal level of $[Ca^{2+}]_{in}$. Although the RMP of HEK-293 cells covers a large range (−50 to −20 mV), our data strongly suggest that the increase in the basal level of $[Ca^{2+}]_{in}$ occurs in association with the window current of T-channels. Recently, Sutton et al. [23] demonstrated that overexpression of P/Q-type Ca^{2+} channels in HEK-293 cells can mediate an elevation of resting $[Ca^{2+}]_{in}$ responsible for syntaxin-1A expression. Similarly, we suggest that T-channels play an important role by tuning $[Ca^{2+}]_{in}$ and therefore could participate to the regulation of Ca^{2+}-dependent pathways, including gene expression.

The factors regulating the functional expression of T-type Ca^{2+} channels have yet to be identified. Beside defining the exact role of T-channels in cell cycle progression, it will be important to identify the cell cycle-dependent pathways involved in the functional expression of T-channels. These regulations could occur at specific stages of development and pathogenesis, and most probably are cell type-dependent. The association of $I_{Ca,T}$ with cellular proliferation is well documented for vascular smooth muscle (VSM) myocytes [7,8,28,29] and it will now be important to determine whether the overexpression of T-channels in VSM cells modulate cell proliferation. The data reported here have demonstrated that basal $[Ca^{2+}]_{in}$ can depend on T-channel expression. This observation is important to consider since concomitant T-channel expression and Ca^{2+} overload have been reported in cardiovascular diseases, such as cardiac hypertrophy [30,31]. Further investigations should therefore combine manipulation of T-channel expression, $[Ca^{2+}]_{in}$ measurements and analysis of Ca^{2+}-dependent pathways to determine the role of T-channels in normal physiology as well as in pathogenesis.

Acknowledgements: This work was supported in part by the Programme Génome du CNRS, Association pour la Recherche contre le Cancer (No. ARC9011), Association Française contre les myopathies, Fondation de France (Grant 97003982) and a Grant from

Hoescht-Marion-Roussel laboratories (FRHMR1/9702). A.M. was supported by Produit Roche (France) and the Groupe de Réflexion sur la Recherche Cardio-vasculaire.

References

[1] McCobb, D.P., Best, P.M. and Beam, K.G. (1989) Neuron 2, 1633–1643.
[2] Xu, X. and Best, P.M. (1992) J. Physiol. (Lond.) 454, 657–672.
[3] Beam, K.G. and Knudson, C.M. (1988) J. Gen. Physiol. 91, 799–815.
[4] Monteil, A., Chemin, J., Bourinet, E., Mennessier, G., Lory, P. and Nargeot, J. (2000) J. Biol. Chem. 275, 6090–6100.
[5] Day, M.L., Johnson, M.H. and Cook, D.I. (1998) Pfluegers Arch. 436, 834–842.
[6] Rohwedel, J., Maltsev, V., Bober, E., Arnold, H.H., Hescheler, J. and Wobus, A.M. (1994) Dev. Biol. 164, 87–101.
[7] Richard, S., Neveu, D., Carnac, G., Bodin, P., Travo, P. and Nargeot, J. (1992) Biochim. Biophys. Acta 1160, 95–104.
[8] Kuga, T., Kobayashi, S., Hirakawa, Y., Kanaide, H. and Takeshita, A. (1996) Circ. Res. 79, 14–19.
[9] Guo, W., Kamiya, K., Kodama, I. and Toyama, J. (1998) J. Mol. Cell. Cardiol. 30, 1095–1103.
[10] Chen, C.F., Corbley, M.J., Roberts, T.M. and Hess, P. (1988) Science 239, 1024–1026.
[11] Wang, Z., Estacion, M. and Mordan, L.J. (1993) Am. J. Physiol. 265, 1239–1246.
[12] Schmitt, R., Clozel, J.P., Iberg, N. and Buhler, F.R. (1995) Arterioscler. Thromb. Vasc. Biol. 15, 1161–1165.
[13] Liu, J.H., Bijlenga, P., Occhiodoro, T., Fischer-Lougheed, J., Bader, C.R. and Bernheim, L. (1999) Br. J. Pharmacol. 126, 245–250.
[14] Welker, H.A., Wiltshire, H. and Bullingham, R. (1998) Clin. Pharmacokinet. 35, 405–423.
[15] Perez-Reyes, E., Cribbs, L.L., Daud, A., Lacerda, A.E., Barclay, J., Williamson, M.P., Fox, M., Rees, M. and Lee, J.H. (1998) Nature 391, 896–900.
[16] Cribbs, L.L., Lee, J.H., Yang, J., Satin, J., Zhang, Y., Daud, A., Barclay, J., Williamson, M.P., Fox, M., Rees, M. and Perez-Reyes, E. (1998) Circ. Res. 83, 103–109.
[17] Williams, M.E., Washburn, M.S., Hans, M., Urrutia, A., Brust, P.F., Prodanovich, P., Harpold, M.M. and Stauderman, K.A. (1999) J. Neurochem. 72, 791–799.
[18] Lee, J.H., Daud, A.N., Cribbs, L.L., Lacerda, A.E., Pereverzev, A., Klockner, U., Schneider, T. and Perez-Reyes, E. (1999) J. Neurosci. 19, 1912–1921.
[19] Monteil, A., Chemin, J., Leuranguer, V., Altier, C., Mennessier, G., Bourinet, E., Lory, P. and Nargeot, J. (2000) J. Biol. Chem. 275, 16530–16535.
[20] Wang, L.D., Hoeltzel, M., Butler, K., Hare, B., Todisco, A., Wang, M. and Delvalle, J. (1997) Am. J. Physiol. 273, 2037–2045.
[21] Stepan, V.M., Krametter, D.F., Matsushima, M., Todisco, A., Delvalle, J. and Dickinson, C.J. (1999) Am. J. Physiol. 277, 572–581.
[22] Biard, D.S., Kannouche, P., Lannuzel-Drogou, C., Mauffrey, P., Apiou, F. and Angulo, J.F. (1999) Exp. Cell. Res. 250, 499–509.
[23] Sutton, K.G., McRory, J.E., Guthrie, H., Murphy, T.H. and Snutch, T.P. (1999) Nature 401, 800–804.
[24] Brideau, A.D., Banfield, B.W. and Enquist, L.W. (1998) J. Virol. 72, 4560–4570.
[25] Kalejta, R.F., Brideau, A.D., Banfield, B.W. and Beavis, A.J. (1999) J. Exp. Cell. Res. 248, 322–328.
[26] Takagi, S., McFadden, M.L., Humphreys, R.E., Woda, B.A. and Sairenji, T. (1993) Cytometry 14, 640–648.
[27] Lee, J.H., Gomora, J.C., Cribbs, L.L. and Perez-Reyes, E. (1999) Biophys. J. 77, 3034–3042.
[28] Neveu, D., Nargeot, J. and Richard, S. (1993) Pfluegers Arch. 424, 45–53.
[29] Richard, S. and Nargeot, J. (1998) in: Low-voltage-activated T-type Calcium Channels (Tsien, R.W., Clozel, J.P. and Nargeot, J., Eds.), pp. 123–132. ADIS International, Chester.
[30] Nuss, H.B. and Houser, S.R. (1995) Circ. Res. 73, 777–782.
[31] Martinez, M.L., Heredia, M.P. and Delgado, C. (1999) J. Mol. Cell. Cardiol. 31, 1617–1625.